Stability analysis in an inverter-dominant microgrid facing in-rush current of an induction machine

Nastaran Fazli, David Hammes, Sidney Gierschner, Hans-Günter Eckel
Institute of Electrical Power Engineering
University of Rostock
Rostock, GERMANY
Phone: +49 381 498-7115
Email: nastaran.fazli@uni-rostock.de

Acknowledgments

This paper was made within the framework of the research project "OffWiPP", which is supported by the Federal Ministry for Economic Affairs and Energy (03El4037A) on the basis of a decision by the German Bundestag.

Keywords

≪Grid-forming converters≫, ≪Renewable energy systems≫, ≪Induction motor≫, ≪Islanded operation≫, ≪Power system stability≫.

Abstract

In islanding operation with high shares of renewables, transient disturbances may put the system in danger of instability. In such a situation, the frequency-voltage profile of the remaining power system, does not only depend on the depth of the unbalance, which appears following a transient, but also to the percentage of renewables and their control topologies as well as the dominant load on the islanded area. Hence in this paper, the renewables are controlled to act as a grid-supporting current and voltage sources. Also the load characteristic is varying from dominant resistive, to dominant induction machine and converter- fed loads. The emergency measures for under- and over-frequency and voltage control is also considered the same in all simulation scenarios. The simulations are carried out in Matlab-Simulink via different scenarios to find out if the islanded power system and the generation units in that area are able to handle such a transient event considering different criteria via the emergency measures in the islanded power system.

Introduction

With continues growth of non-synchronous generation (NSG) units, following the trend of decarbonizing the globe, the share of renewable energy sources (RES) reached to an alarming level regarding power system security. In addition to the reduction of power system strength including mechanical inertia and short-circuit ratio with growing of NSGs, an investigation in 2013 shows that control interaction and instability of these units in higher shares is another issue which has to be considered [1].
On the other hand, the pressure on the installed equipment of the actual power system has increased the risk of events leading to system splits within continent Europe in recent years [2]. There are mainly two threats for an unintentional islanding event according to [3], first one refers to the the high unbalances after islanding, and the second one to the amount of inertia in the islanded area, that this work focus on the second part. Additionally, in the remaining power

system after separation, stability does not only depend on the share of NSG to the conventional synchronous generator (SG) units but also to the load combination in this area [4].
Industrial loads for example with a high share of induction machines (IM) can have a different characteristic in response to the disturbances than residential load with more share of heating, lighting and converter-fed loads, as they don't share the frequency-supporting features of a directly-connected drive [5]. In addition to it, are the disturbances like turning on a huge IM or tripping transmission lines and etc, which affects frequency and voltage stability on the power system. This can drag the system towards instability border and cascading events especially if the system is separated from a bulky part of the power system and if SGs of that area are reaching their operational limits to support the power system with active power injection and reactive power supplying.
As mentioned in [2], the seven main concerns of power system operators, can nowadays be supported by grid-supporting voltage source (GSVS) control of converters. These types of control for a voltage source inverter (VSI) can emulate similar behavior to an SG by providing instantaneous reserve or inertia support and voltage control as much as their limitation on available energy, actual operating point and over current capability allows. By increasing share of RES, the task is to find out the border of how much state-of-the-art grid-supporting current source (GSCS)is required to be replaced by GSVS to ensure system stability. This depends on many criteria, namely, for which unbalances GSVS should be dimensioned, future speed of triggering under-frequency load shedding (UFLS) relays, if primary control is provided by RES and lastly to the load composition and taking into accounts transients which may occur during islanding of the power system.
Starting up of a huge IM is one of these transients that can drag an islanded power system to the border of instability. As during starting, the IMs draw a high current duo to their lower machine impedance in lower speed of the rotor if they are not compensated [6]. This will place the system especially with high shares of renewable to a alarming stage as the majority of the installed capacity of RES don't have an instantaneous reaction to such disturbances. However, the GSVSs will inherently sense these voltage and frequency variations and can participate in counteracting their effect.
Therefore, the effect of the inrush current of an IM during islanding is going to be investigated. In this paper, a similar power unbalance via hard start of an IM is going to be tested via different scenarios. The frequency–voltage stability in the islanded area will be evaluated using also the emergency measures like limited frequency sensitive mode – underfrequency (LFSM-U) and limited frequency sensitive mode – overfrequency (LFSM-O), voltage-var control and under-voltage load sheeding (UVLS). Among all the other participating factors like percentage of unbalances, how slow is the LFSM-O with limitation of conventional units and how fast are LSRs and etc, the focus in this paper is drawn to investigate the minimum required inertia with looking at the effect of the dominant load classes in this microgrid during the event.

Structure of the Power System

The power system structure is taken from the model of Kundur [7], as shown in Fig.1. The wind turbines (WT) of the available RES are a mixture of GSCSs and GSVSs.

RESs Control Strategy

In order to provide grid-supporting features and to fulfill grid requirements, the control of a branch of RESs in Fig.1 is realized via Grid-supporting current source (GSCS), which is an extension of the state-of the-art grid following current source converter. The GSCS is implemented in a power converter with voltage-oriented control, which controls the converter currents in the inner loop [8] and active and reactive powers in the slower outer loop. A Phase-locked loop (PLL) is used for grid synchronization and current limitations is applied on the controller current references to protect the converter semi-conductor switches. In the other branch of RES, a GSVS is applied using Rotating-voltage-vector control (RVVC) [12]. The active power loop

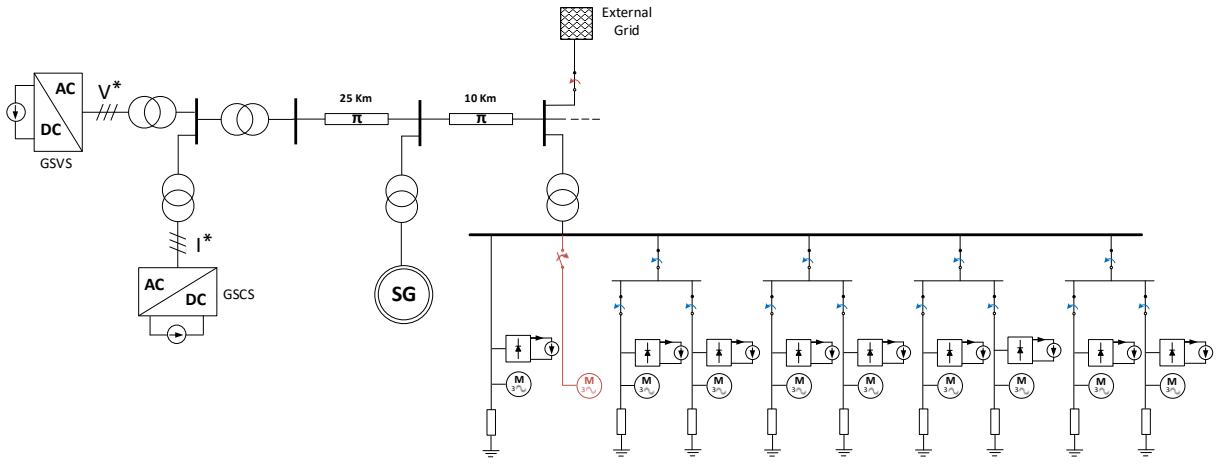

Fig. 1: Model of the simulated power system

uses the mechanical inertia constant in a similar way to a SG. The converter filter impedance is $\mathbf{x}_{\mathrm{f}} = 0.01$ pu and its inertia constant is H=5 s. Instantaneous reserve is realized via active power loop to support the grid frequency deviation and provide time for the containment reserve and load shedding relays (LSRs) to act. Primary control is also a choice of system operator and can be activated if WT is operating in sub-optimal curve [13]. A DC-link voltage controller is realized in the machine-side converter control to guarantee a steady DC voltage when grid frequency and voltage changes. This is done by varying the torque of permanent magnet synchronous generator of WT depending on the depth of frequency fall and choice of parameters in GSVS. Over-current limitation will be triggered when the currents go beyond 1.2 pu limit.

Synchronous Generator (SG)

An SG is used with an speed governor and active voltage regulator (AVR) using the SM AC2C excitation system in conformation with IEEE [14]. The transient impedance of SG is $\mathbf{x'}_{\mathrm{d}} = 0.1$ pu similar to GSVS filter and Mechanical inertia is H = 5 s similar to GSVS at nominal power.

Loads

Five main branches of load is realized in the simulated power system, as shown in Fig.1. Four branches, are each comprised of 12.5% of the total load power and the rest 50% is in the last branch. Each branch has a mixture of resistive loads (resembling heating and lighting loads), directly-connecting machines (IMs) and converter-connected drives (B6U). The proportion of each type of the load relative to the other types is verying in different simulation scenarios based on [5] to show a fraction of typical loads in residential, commercial or industrial area. According to the Fig. 2-4 of [5], a hypothesis of the load composition for three different load classes is considered as follows: in the class I, similar to the residential area that normally heating and cooking power consumption is high, a dominant share of resistive load 50%, 30% IM and 20% B6U is considered. The load Class II belongs to the industrial area, where majority of loads are motors. In this class, a share of 70% IM, 20% B6U and lastly 10% resistive loads is considered. And the load class III, is the situation when a high share of converter-connected drives exist. The loads in this class are 50% B6U, 30% IM, and 20% resistive load.

Emergency remedies including LFSM-O, LFSM-U, Voltage control, UFLS and UVLS

The LFSM-O is applied for both GSCS and GSVS converters with a time constant of 1.7 s to fulfill the grid requirements regarding over-frequency power reduction [9], [10]. According to

Table I: Simulated Scenarios

Load class I		Load Class II		Load Class III	
50% Resistive- 30% IM- 20% B6U		10% Resistive- 70% IM- 20% B6U		20% Resistive- 30% IM- 50% B6U	
Test 1	100% SG	**Test 2**	100% SG	**Test 3**	100% SG
Test 4	50% SG- 50% GSCS	**Test 5**	50% SG- 50% GSCS	**Test 6**	50% SG- 50% GSCS
Test 13	50% SG- 25% GSCS- 20%GSVS	**Test 14**	50% SG- 25% GSCS- 20%GSVS	**Test 15**	50% SG- 25% GSCS- 20%GSVS
Test 7	25% SG- 90% GSCS	**Test 8**	25% SG- 90% GSCS	**Test 9**	25% SG- 90% GSCS
Test 16	25% SG- 37.5% GSCS- 37.5%GSVS	**Test 17**	25% SG- 37.5% GSCS- 37.5%GSVS	**Test 18**	25% SG- 37.5% GSCS- 37.5%GSVS
Test 10	10% SG- 90% GSCS	**Test 11**	10% SG- 90% GSCS	**Test 12**	10% SG- 90% GSCS
Test 19	10% SG- 45% GSCS- 45%GSVS	**Test 20**	10% SG- 45% GSCS- 45%GSVS	**Test 21**	10% SG- 45% GSCS- 45%GSVS

these regulations, LFSM-O will be activated from 50.2 Hz with a droop slope of -20 pu to drop 50% of the generation when the frequency reaches to the threshold of tripping units (51.5 Hz). For SG, however, the LFSM-O is applied with a bigger time constant (8 s) due to limitations for conventional units that requires a slower reaction [11].

A voltage droop controller is also applied for both GSCS and GSVS according to grid connection standards [11]. Based on these regulations, the controller gain is chosen -2 pu and the time constant of the voltage controller's low-pass filter is chosen 10 ms. Based on these parameters, in 50% voltage drop, RESs will deliver 1 pu of overexcited reactive power within 30 ms. The dead-band for activation of the voltage controller is ±5% of nominal voltage. For SG, a similar deadband is applied to the AVR. Also, the reactive power of SG is limited to 1 pu of the nominal apparent power by under excitation and over excitation limiting controllers.

The LFSM-U refers to the activation of the frequency containment reserves (FCR) when the system is in an emergency state in underfrequency events. This is only realized via SG here, as the RESs are designed to operate in maximum power point. The same limiattion of LFSM-O for power reduction is applied here for LSFM-U with SG. That SG can ramp the power with a rate limited to 20% min^{-1}.

The other emergency action is under-frequency load shedding (UFLS). These relays are located in four branches to be able to disconnect each time 12.5% of the total load at frequency thresholds of f= {49-48.8-48.6-48 Hz} as a last defense action for keeping stability in the power system. At each of these thresholds, the frequency has to stay below this value for four consecutive grid cycles until the tripping signal is sent and then there will be another 100 ms delay from the emitted signal until the relays opens up and disconnect the load. The Under voltage load shedding (UVLS) relays are also placed in eight sub-branches of the loads as a counter-measure action against voltage dips in an area. Load characteristic plays an import role in UVLS. For instance, voltage-dependent loads like resistive loads don't necessarily need a prompt reaction when under voltage happens, IMs, however, need a less delayed reaction from under voltage relays (around 1.5 s) [15]. Therefore a faster load shedding concept here is considered. Each UVLS relay drops 6% of the total load in the following time stamps [15] : -10% below nominal voltage with 1.5 s time delay, -10% below nominal voltage with 3 s time delay, -10% below nominal voltage with 5 s time delay.

Simulation Scenarios

The question of how much GSVSs is necessary to bring back the strength to the actual power system is being investigated in some optimistic and pessimistic studies [4] and [17]. In these concepts, grid following current sources are replaced by GSVSs to mitigate the concern of TSOs regarding system security. However, in most studies the influence of consumer side is not considered. In [16], this effect is partially being seen on the islanding event in Flensburg in 2019. Therefore, in this paper, first the line connecting the power system to the external grid is disconnected some ms before t= 0 s and then at t= 0 s, the starting process of a high power IM (with a nominal power equal to 4% of the total load), without any compensation is studied in different islanding scenarios with high RES and the three classes of loads. The results of some of

these test scenarios are shown and compared in the following. The criteria for the analyzing test scenarios is that frequency and voltage stay inside normal operating band (f = [47.5 - 51.5 Hz] and V = ±10%), also using remedial measures. Another important criteria here is the Rate of Change of Frequency (ROCOF) and the number of needed load shedding (LS) before reaching to a new steady state value. Importance of ROCOF criteria is because the value of ROCOF is often used along with a threshold value for a fast UFLS. Also a high ROCOF can lead to malfunctioning of protection relays that are installed in medium voltage grid to detect islanding. According to [18], the setting for these relays are normally between 0.1 - 1.0 Hzs^{-1}. On the other hand, ROCOFs higher than -1 Hzs^{-1} not only can lead to malfunctioning of emergeny equipments in the power system, but also it might cause instability and lifetime threats for conventional generation units. Hence, in this work, ROCOF rate of -1 Hzs^{-1} is considered critical in choosing minimum required inertia to stand such a transient.

Comparing Load Classes I-III in the Base Scenario

Fig. 2 shows and compares the results of starting an IM at t = 0 s in different classes of loads with base scenario, where there is not any RESs participating in the generation. This is shown by T1 and 2 and 3 in Fig.2, (*T stands for the word test*). In all tests, voltage stability is assured thanks to fast voltage support of the SG. The voltage stays within ±10% Vn which is the allowed operation band. The best df/dt among these three tests belongs to T1 with highest percentage of resistive load. This is achieved because the voltage has droped with starting of IM, and as a result, resistive loads with quadratic relation with the supply voltage, have reduced their active power consumption. In this case, by reduction of ΔP, df/dt gets smoother and reaches a value of -0.38 Hzs^{-1} measured in a window of 500 ms. However, by recovery of the voltage, the ΔP also increases and ends up with activation of first step of LS after 7.2 s.

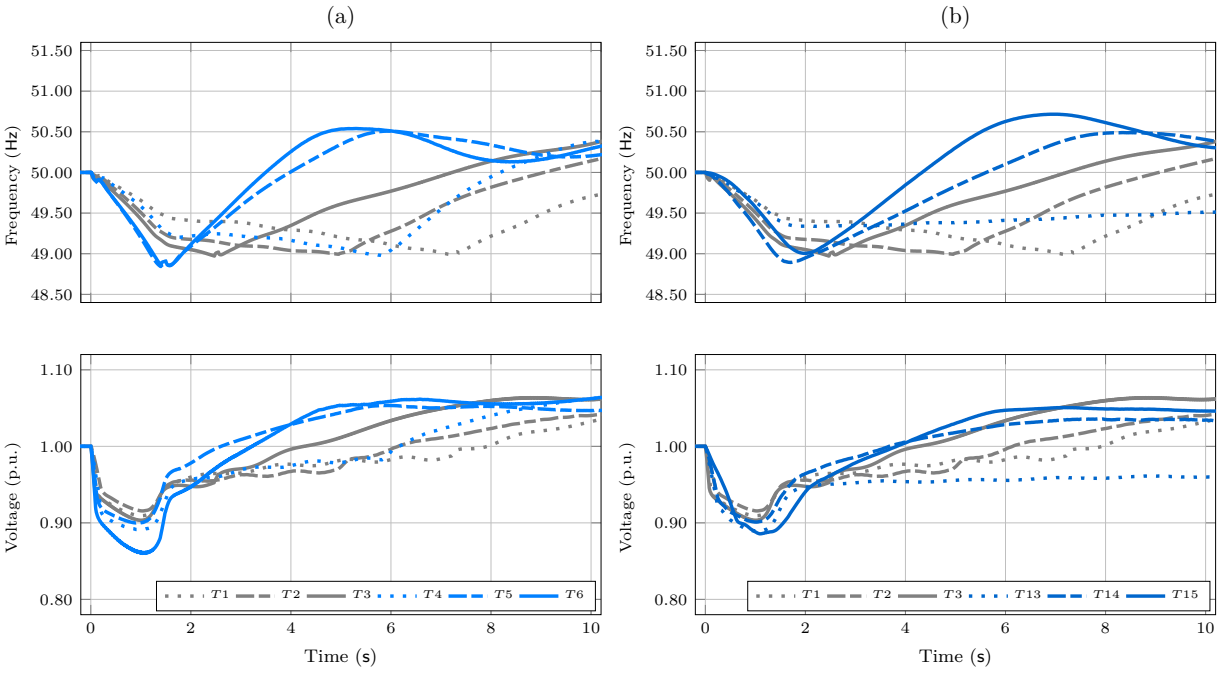

Fig. 2: Base tests with only SG are shown in gray. a) Tests with having SG+GSCS in Generation side are shown in light blue, b) Tests with having SG+ GSCS+ GSVS in generation side are shown in dark blue

In T2, with turning on process of IM, the voltage drops, however, not as low as the T1 and T3 due to high proportion of IM. The load of IM in the consumer side is a variable-torque load, whose mechanical torque is a function of square of rotational speed. Therefore, with reduction

Table II: Detail of test results in Fig.2

Tests	F min (Hz)	F max (Hz)	ROCOF (Hz/s)	Number of LS	LS time (s)	Vmin (pu)	Vmax (pu)
T1	49.00	50.40	0.38	once	7.20	0.91	1.06
T2	49.00	50.65	0.38	once	5.00	0.92	1.05
T3	49.00	50.70	0.38	once	2.47	0.90	1.07
T4	49.00	50.80	0.48	once	5.81	0.89	1.06
T13	49.35	49.60	0.40	none	-	0.89	0.96
T5	49.00	50.50	0.76	once	1.38	0.90	1.05
T14	49.00	50.49	0.75	once	1.57	0.90	1.03
T6	49.00	50.56	0.75	once	1.39	0.86	1.06
T15	49.00	50.70	0.64	once	1.67	0.88	1.05

of the voltage, the other IMs in the consumer side, have decreased their electrical torque as a function of the grid voltage and proportionally their rotational speed, and with that their power consumption has dropped. In this condition, the power factor of the load improves and this improves the voltage profile in the power system with load class II. The df/dt in T2 is slightly better than T3. It is also shown that by bringing back the voltage of T2 and T3, into the normal operating band, frequency starts deviating more in T3 comparing to T2 due to higher resistive loads and less self-regulating effect. Therefore, the fastest LS happens with T3 (after 2.47 s) and then it follows by T2 (after 5 s). In general, in all T1-3, the grid can keep the voltage stability and frequency stability after such a transient by only one step of load shedding. The details about test results is summarized in Table II.

In T4, 50% of the load power is generated from the RES with GSCS. Among T4-6, voltage stability is only maintained for T5 with IM dominant loads. The df/dt in all cases is worsen due to higher share of RESs in the generation side. Still T4 has the best df/dt as the voltage drops even lower than T1. The value of df/dt is slightly lower in T5 comparing to T6. Therefore, a faster load shedding happens with T5 after (1.38 s).

Comparing T4 versus T13 shows that both reach to a minimum voltage of below 0.9 pu. However, in contarst to T4 with GSCS, in T13 the effect of inertia support from GSVS is shown. As with almost similar voltage profile after the event, the ROCOF has improved and the frequency settles in a new equilibrium point without the need for load shedding in T13, in contrast to T4 that load shedding is happening after 5.81 s. Comparing T5 versus T14, shows an acceptable voltage support in both scenarios. In a similar way, df/dt is improved in T14 and this results in a delayed LS comparing to T5. In T15, voltage support from both SG and GSVS can result in a better voltage profile in contrast to voltage in T6. The oscillation in the voltage of T15 comes from over-current activation to protect GSVS from over-currents due to huge active and reactive power support. Again a better inertia support is seen with T15.

Comparing Generation Combinations in Load Class III

Fig. 3 shows the simulation results of another group of tests which have the same class of load (Class III) but their generation unit is changing in the percentage of SG and RESs with and without GSVS. As it is shown in Fig. 3(a), by increasing the share of RESs from T9 to T12, how much negative ROCOF decreases due to reduction of inertia in the islanded power system. The decrease of df/dt from -1.03 $\mathrm{Hz\,s^{-1}}$ in T9 to -1.6 $\mathrm{Hz\,s^{-1}}$ in T12 causes triggering of the first load shedding relay very fast after 0.68 s. In both tests (T9 and T12), 24% of the load has dropped in two steps of load shedding behind each other. When 50% of the RESs is replaced by GSVS in T18 and T21, the results shows that the ROCOF has improved. This is shown by Fig. 3(c) and (e) that facing the inrush current of the IM during islanding, causes a frequency deviation,

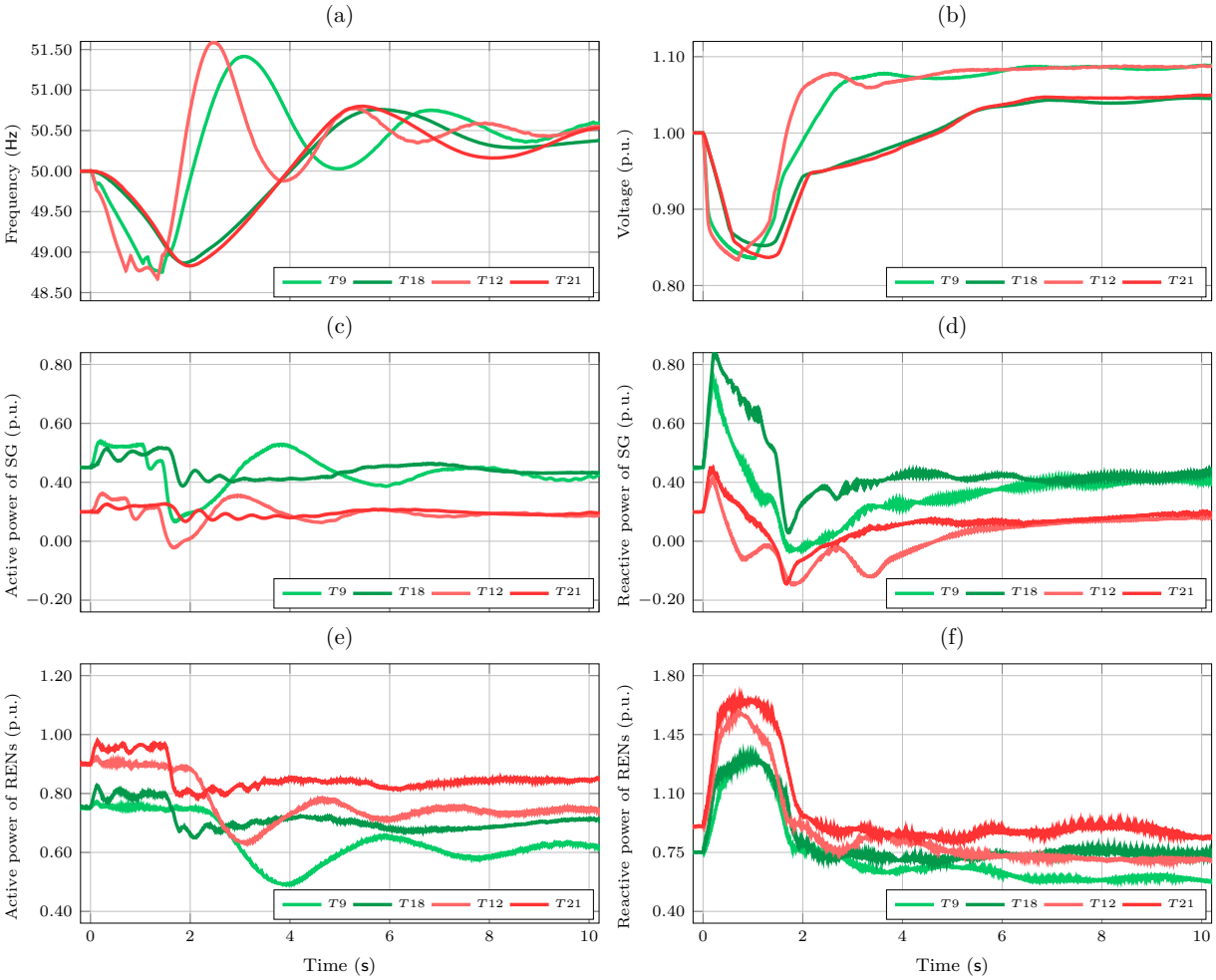

Fig. 3: a) frequency, b) voltage at the load bus, c) Active power of SG, d) reactive power of SG, e) active power of RESs including GSCS & GSVS, f) reactive power of RESs including GSCS & GSVS

due to ΔP in the islanded system. As a result, there is a deviation in the frequency that in T9 & T12, only SG is counteracting it (Fig.3(c)). Reducing the share of SG from 25% (T_G=2.5 s) to 10% (T_G=1 s), causes a steeper ROCOF once the IM is turning on. In contrast, in T18 with GSVS which has a 50% share of the RESs (T_G=6.2 s), a higher inertia can be provided via generation units comparing to T9. As it is shown in Fig.3(c), the SG doesn't compensate only for the frequency deviation, also RESs are participating in inertia power. In the similar manner is T21 (T_G=5.5 s), although the time constant has dropped comparing to T12, the frequency and voltage stability improved comparing to the similar cases with T9 and T12. The details about test results is summarized in Table III.

After deceleration phase, and activation of first step of load shedding, the frequency rises again into over-frequency region. As it is shown with T12, the frequency goes from normal frequency band to the band that normally generation units disconnect from the power system [3]. This is critical in this way that according to the data of historic events [16], separation of generation units can cause cascaded events and can end up with blackout. Therefore, in T12, the amount of inertia is insufficient in facing such transients. In other tests, the frequency stays in the allowed frequency band. In over-frequencies, LFSM-O of all RESs and SG are participating in curtailing their power. However, from the moment that df/dt becomes positive, the reaction of SG and GSVS is almost intrinsic due their voltage source nature. This reduces +Δp in the system. On the other hand, for RESs with current source nature, the LFSM-O starts reducing the active

Table III: Detail of test results in Fig.3

Tests	F min (Hz)	Fmax (Hz)	ROCOF (Hz/s)	Number of LS	LS time (s)	Vmin (pu)	Vmax (pu)
T9	48.80	51.43	1.03	twice	1.04 - 1.43	0.83	1.08
T18	49.00	50.76	0.65	once	1.65	0.85	1.04
T12	48.80	51.60	1.60	twice	0.70 -1.33	0.83	1.08
T21	49.00	50.80	0.67	once	1.51	0.83	1.04

power only when the frequency passes 50.2 Hz which is the threshold value for activation of LFSM-O. This delayed reaction of GSCS comparing to SG and GSVS is shown in Fig.3(c) and (e) between T9 and T18. After 2nd load shedding, and with positive ROCOF, SG and GSVS both absorbed additional power in the system, however, GSCS power reduction starts more than 0.5 s later. Due to this slower reaction and dropping two branches of the load, the frequency rises the most in T12 (out of the allowed band). The over-frequencies are smaller due to max 12% load shedding in both T18 and T21 and also faster reaction from the generation units.

Looking at voltage profiles, the reduction in SG share has reduced the voltage from T9 to T12. This is due to inherent voltage source nature of the SG that reacts immediately to variation of voltage in its terminal. GSCS, however, with the droop controller reacts to the voltage variation once the voltage has passes the dead band of ±5% and with a time constant of 0.01 s. The RESs with GSVS on the other hand, have an intrinsic response to the voltage variation in the bus they are connecting to it. As the results show for the load class III, when the percentage of B6U is high in the load combination, with starting the inrush current of the IM, due to huge reactive current at the starting, the voltage drops hugely.

In this load type, a huge reactive current is drawn, when the voltage is dropping, in order to keep the active power constant. Hence, the reactive power consumption via the passive elements and filter of the B6U slightly increases. Converter-fed loads, in general, in case of the frequency variation don't participate in frequency-dependent active power reduction, in contrast to IMs, and in case of voltage fall, B6Us don't support voltage by reduction of reactive power consumption as well. Therefore, the voltage profile is the worst with converter-dominant loads.

Comparing Classes II-III in Various Generation Combinations

These series of simulation results are shown in Fig. 4. Comparing T9 and T12, shows that the negative ROCOF is slightly lower in Converter-dominant load, comparing to the IM dominant loads. So with both cases of T9 and T12, a faster load shedding is happening due to steeper ROCOF. In T12, the frequency goes out of allowed operation band and doesn't stay within stable borders. In all tests 9-12, the voltage is below normal operation band and after an under frequency load shedding and with voltage support from generation units, it is taken back to the allowed band without the need for UVLS. To compare these results with their equivalent tests (T17-21) when 50% of RES generation is provided via GSVSs, it is shown obviously that df/dt is improved in all tests of T17-21. Needing only one step of load shedding and a slight voltage improvement is due to support from GSVSs. The details about test results is summarized in Table IV. The difference between frequency profile between Fig. 4(a) and (b) shows that the ROCOF is steeper with Class II in contrast to Class III, when GSVSs have 50% of the RESs. The reason for this can be due to voltage supporting functionality of the GSVS RESs, that the voltage profile has improved in tests 17-21 comparing to the equivalent tests of 8 -12, with this difference that a very fast load shedding didn't drop the loads at very beginning similar to tests 8-12. Therefore, the results show that in T18 and T21 before any load shedding happens, the voltage profile goes so low that the remaining loads of the load class III, will reduce even further their power consumption (Resistive and IM loads). Therefore, in contrast to T17 and T20, the low voltage profile has helped the frequency deviation and T17 and T20, got a steeper df/dt

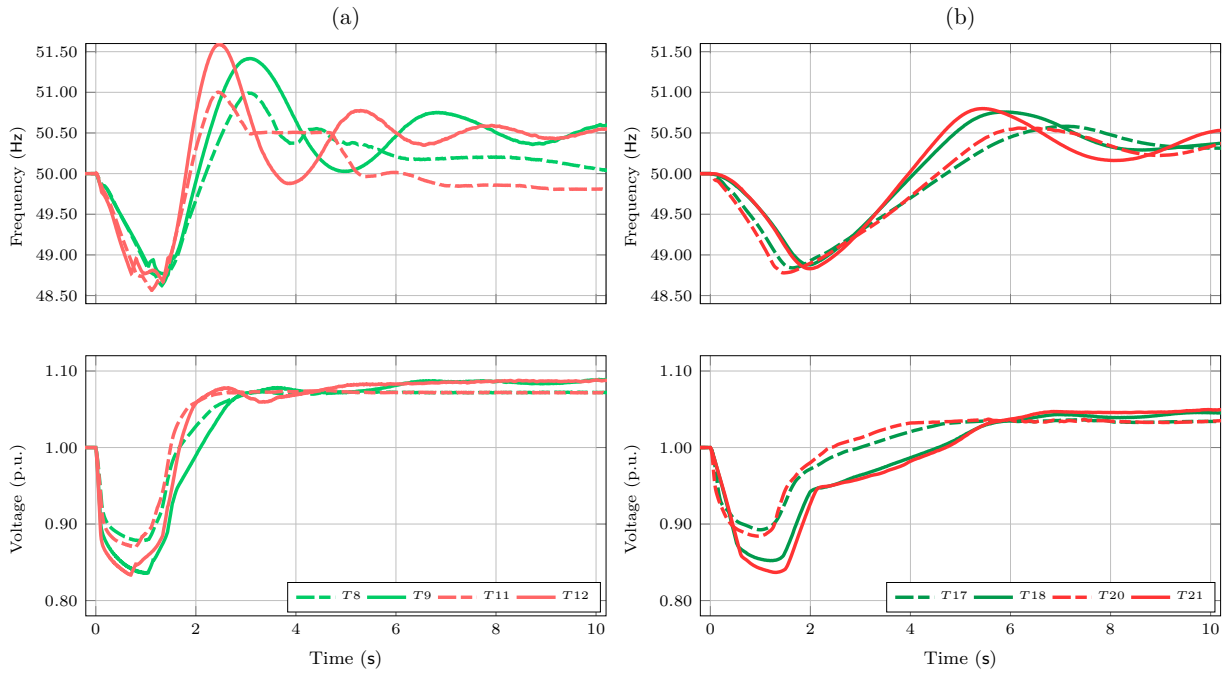

Fig. 4: a) Tests with having SG+GSCS in Generation side in light green and red, b) Tests with having SG+ GSCS+ GSVS in generation side in dark green and red

Table IV: Detail of test results in Fig.4

Tests	F min (Hz)	Fmax (Hz)	ROCOF (Hz/s)	Number of LS	LS time (s)	Vmin (pu)	Vmax (pu)
T8	48.80	50.98	1.04	twice	1.06 - 1.31	0.88	1.07
T17	49.00	50.58	0.76	once	1.50	0.89	1.03
T9	48.80	51.41	1.03	twice	1.04 –1.43	0.83	1.06
T18	49.00	50.76	0.65	once	1.65	0.85	1.04
T11	48.80	51.00	1.50	twice	0.8 – 1.11	0.87	1.07
T20	49.00	50.56	0.88	once	1.24	0.88	1.03
T12	48.80	51.60	1.60	twice	0.70 -1.33	0.83	1.08
T21	49.00	50.80	0.67	once	1.51	0.83	1.04

and a faster load shedding comparing to T18 and T21 with dominant B6U. Also we can see that ROCOF has improved from -1.04 Hzs^{-1} in T8 to -0.76 Hzs^{-1} in T17. The same trend exist between T9 and T18. In both T17 and T18 a ROCOF above -1 Hzs^{-1} was resulted from deploying GSVSs in RESs. Also, the number of LS in Fig.4(a) doesn't increase from one step in contrast to Fig. 4(b) that in all tests two steps of load shedding is necessary and still the power system is not in the stable border, for instance in T12. Looking at the voltage profile at T9, shows that the voltage has dropped the most with load class III. As B6U will increase slightly the reactive power consumption due to its filter when the grid voltage is below rated value. This worsens the voltage profile comparing to load class II, because the IMs are feeding a variable torque load. In this case, IMs decreases the electromagnetic torque as a function of source voltage. This decelerates the IM and the active and reactive power consumption of the load is decreasing proportional to the square of the speed. Because of that, as it is shown, the voltage in T8 & T11 and T17 & T20 is higher than the ones in load class III.

Conclusion

Comparing different scenarios showed a grid dominant by the resistive load offers the best voltage-dependent active power reduction, when following the inrush current from IM, a huge reactive current is drawn which deteriorates the voltage profile in the load bus. If the main load is IM, depending on their connecting load, they could offer the best grid-supporting characteristics with self-regulation effect and voltage-dependent power consumption variation. Hence, the best voltage profile was seen with this load class in all test scenarios. And lastly, when converter-fed loads are dominant in the consumer side, it was shown that grid-friendly features of IMs have vanished. Instead, in order to keep the active power consumption constant, when the voltage has fallen, a converter-fed drive increased the current flow and with that, reactive power consumption was increased. This was shown by the voltage profile in all cases with dominant B6U in the consumer side.

Looking at the results for different share of non-synchronous generation units, showed that above 50% RESs, in all cases except load class I, the power system is not able to stay stable unless 50% of RESs are replaced by GSVS. Replacing GSCS with GSVS, in almost all cases, has improved either ROCOF, delayed, eliminated or reduced the number of consecutive load shedding and improved voltage profile. Even with 90% RES, the ROCOF stayed above -1 $\mathrm{Hz s^{-1}}$, which is critical especially if the equipment for remedial actions in the power system are exhausted or old to deal with such unbalances in the islanded area. The results in this paper showed the necessity of considering the dominant load characteristic to hold up an islanding condition even facing transient events. These results in the small scale has shown another factor which plays a critical role in studying minimum required inertia in the power system.

References

[1] H. Urdal, R. Ierna, J. Zhu, C. Ivanov, A. Dahresobh, et al., "System strength considerations in a converter dominated power system," in 12th Wind Integration Workshop, London, England, 2013.

[2] ENTSO-E, "High Penetration of Power Electronic Interfaced Power Sources and the Potential Contribution of Grid Forming Converters," Technical Report, 2020.

[3] D. Duckwitz, "Power System Inertia Derivation of Requirements and Comparison of Inertia Emulation Methods for Converter-based Power Plants," Ph.D dissertation, Electrical Engineering and Computer Science of the University of Kassel, 2019.

[4] N. Fazli, S. Gierschner and H.-G. Eckel, "Evaluating frequency stability with consideration of load type in different share of renewables and emulated inertia in case of system split," 22nd European Conference on Power Electronics and Applications (EPE'20 ECCE Europe), 2020.

[5] "Modelling and Aggregation of Loads in Flexible Power Networks- Working Group C4.605- Report 566," 2014.

[6] P. J. Colleran and W. E. Rogers, "Controlled Starting of AC Induction Motors," in IEEE Transactions on Industry Applications, vol. IA-19, no. 6, pp. 1014-1018, Nov. 1983.

[7] Kundur, P."Power System Stability and Control", New York, USA: McGraw- Hill, Inc., 1994. 1776p. ISBN: 0-07-035958-X.

[8] R. Teodorescu, M. Liserre and P. Rodríguez. "Grid Converters for Photovoltaic and Wind Power Systems."(2011).

[9] VDE / FNN, "VDE-AR-N 4120:2015-01 Technical requirements for the connection and operation of customer installations to the high-voltage network (TCC High-Voltage)," 2015.

[10] European Commission, "Commission Regulation (EU) 2016/631 of April 2016 establishing a network code on requirements for grid connection of generators," 2016. [Online]. Available:

http://eur-lex.europa.eu/eli/reg/2016/ 631/oj.

[11] "VDE-AR-N 4120 (draft May 2017) Technical requirements for the connection and operation of customer installations to the high voltage network (TAR high voltage) (German edition)," 2017.

[12] N. Fazli, S. Gierschner, M. Gierschner, L. Cai and H. Eckel, "Rotating-Voltage-Vector Control for Wind Energy Plants Providing Possibility for Ancillary Services," 2018 20th European Conference on Power Electronics and Applications (EPE'18 ECCE Europe), 2018.

[13] Zhang, Z.-S.; Sun, Y.-Z.; Lin, J.; Li, G.-J.: "Coordinated frequency regulation by doubly fed induction generator-based wind power plants", IET Renewable Power Generation, 2012, 6, (1), p. 38-47, DOI: 10.1049/iet-rpg.2010.0208

[14] "IEEE Recommended Practice for Excitation System Models for Power System Stability Studies," in IEEE Std 421.5-2016.

[15] C. W. Taylor, "Concepts of undervoltage load shedding for voltage stability," in IEEE Transactions on Power Delivery, vol. 7, no. 2, pp. 480-488, April 1992.

[16] Thiesen, H, Jauch. C. "Determining the load inertia contribution from different power consumer groups," Energies 2020.

[17] R. Ierna, J. Zhu, H. Urdal, A. J. Roscoe, M. Yu, A. Dysko, and C. D.Booth, "Effects of VSM Convertor Control on Penetration Limits ofNon-Synchronous Generation in the GB Power System," in 15th WindIntegration Workshop, p. 8, Nov. 2016.

[18] H. Kazemi Kargar and J. Mirzaei, "New method for islanding detection of wind turbines," 2008 IEEE 2nd International Power and Energy Conference, 2008.